more freedom of movement for the guest molecules, leading to higher switching rates. Indeed, the persistence times measured for the switches in (*11*) may provide a measure of the order within the nanopore. Molecules that switch remain bound to the same location on the substrate. This group of phenylene ethynylene oligomers, **1′**, **2′**, and **3′**, is qualitatively similar in that they exhibit bistable conductance when inserted into dodecanethiol films; the nitro substituent is not the determining factor in the stochastic conductance switching observed here. We also demonstrated the ability to induce switching, using high electric fields to control the conductance states in **2′**.

References and Notes

1. J. M. Tour, M. Kozaki, J. M. Seminario, *J. Am. Chem. Soc.* **120**, 8486 (1998).
2. J. M. Tour, *Acc. Chem. Res.* **33**, 791 (2000).
3. S. J. Tans, A. R. M. Vershueren, C. Dekker, *Nature* **393**, 49 (1998).
4. C. P. Collier *et al.*, *Science* **285**, 391 (1999).
5. C. P. Collier *et al.*, *Science* **289**, 1172 (2000).
6. J. Chen, M. A. Reed, A. M. Rawlett, J. M. Tour, *Science* **286**, 1550 (1999).
7. J. Chen *et al.*, *Appl. Phys. Lett.* **77**, 1224 (2000).
8. C. Joachim, J. K. Gimzewski, R. R. Schlittler, C. Chavy, *Phys. Rev. Lett.* **74**, 2102 (1995).
9. F. Moresco *et al.*, *Phys. Rev. Lett.* **86**, 672 (2001).
10. D. I. Gittins, D. Bethell, D. J. Schiffrin, R. J. Nichols, *Nature* **408**, 67 (2000).
11. M. A. Reed *et al.*, *Appl. Phys. Lett.* **78**, 3735 (2001).
12. W. E. Moerner, M. Orrit, *Science* **283**, 1670 (1999).
13. X. S. Xie, *Acc. Chem. Res.* **29**, 598 (1996).
14. J. M. Seminario, A. G. Zacarias, J. M. Tour, *J. Am. Chem. Soc.* **122**, 3015 (2000).
15. M. D. Ventra, S. T. Pantelides, N. D. Lang, *Phys. Rev. Lett.* **84**, 979 (2000).
16. J. M. Seminario, A. G. Zacarias, J. M. Tour, *J. Am. Chem. Soc.* **120**, 3970 (1998).
17. P. S. Weiss *et al.*, *Ann. N.Y. Acad. Sci.* **852**, 145 (1998).
18. M. T. Cygan *et al.*, *J. Am. Chem. Soc.* **120**, 2721 (1998).
19. L. A. Bumm *et al.*, *Science* **271**, 1705 (1996).
20. T. D. Dunbar *et al.*, *J. Phys. Chem. B* **104**, 4880 (2000).
21. The SAM matrices were prepared on commercial Au{111} on mica (Molecular Imaging, Phoenix, AZ). The gold substrates were annealed and cleaned with a hydrogen flame immediately before film preparation. SAM matrices were deposited from a 1 mM solution of dodecanethiol in ethanol. The samples were then rinsed in neat ethanol and blown dry with nitrogen. Solutions were prepared that were 0.1 mM of **1**, **2**, or **3** in dry tetrahydrofuran. Aqueous ammonia was added to hydrolyze the acetyl protecting group, generating the thiol in situ to adsorb as the thiolate (**1′**, **2′**, or **3′**) on the surface. The exposure time of the host matrix to the guest molecules typically ranged from several minutes to a few hours. After rinsing and drying, the samples were stored at room temperature in a desiccator. STM imaging was performed under ambient conditions as previously described (*18, 19*).
22. G. E. Poirier, *Chem. Rev.* **97**, 1117 (1997).
23. Movies are available as supplementary material at http://stm1.chem.psu.edu/supplemental/switch.html.
24. Each frame was median filtered. The topographic height was then assigned as the median of the highest nine points in the frame minus the median of the lowest fourth of the extracted image. Thus, an apparent height of 0 would only occur if the image was almost perfectly flat. The extracted frames shown in Fig. 3 were interpolated to twice the pixel density and median filtered.
25. G. E. Poirier, E. D. Pylant, *Science* **272**, 1145 (1996).
26. The annealing process decreases the number of inserted molecules observed in the film. We cannot yet attribute this change to desorption from the film or degradation of the molecules at elevated temperatures.
27. C. F. Herrmann, J. J. Boland, *J. Phys. Chem. B* **103**, 4207 (1999).
28. H. C. Akpati, P. Norlander, L. Lou, P. Avouris, *Surf. Sci.* **372**, 9 (1997).

29. We thank A. Hatzor, P. Lewis, G. McCarty, and R. Smith for experimental assistance and M. Ratner for helpful discussions. The continuing support of the Army Research Office, the Defense Advanced Research Projects Agency, the NSF, the Office of Naval Research, and Zyvex are most gratefully acknowledged.

28 February 2001; accepted 9 May 2001

A 14,000-Year Oxygen Isotope Record from Diatom Silica in Two Alpine Lakes on Mt. Kenya

P. A. Barker,[1] F. A. Street-Perrott,[2] M. J. Leng,[3] P. B. Greenwood,[3] D. L. Swain,[2]* R. A. Perrott,[2] R. J. Telford,[1]† K. J. Ficken[2]

Oxygen isotopes are sensitive tracers of climate change in tropical regions. Abrupt shifts of up to 18 per mil in the oxygen isotope ratio of diatom silica have been found in a 14,000-year record from two alpine lakes on Mt. Kenya. Interpretation of tropical-montane isotope records is controversial, especially concerning the relative roles of precipitation and temperature. Here, we argue that Holocene variations in $\delta^{18}O$ are better explained by lake moisture balance than by temperature-induced fractionation. Episodes of heavy convective precipitation dated ~11,100 to 8600, 6700 to 5600, 2900 to 1900, and <1300 years before the present were linked to enhanced soil erosion, neoglacial ice advances, and forest expansion on Mt. Kenya.

Paleoclimate records from tropical regions are essential to understanding past changes in Earth's climate system, equator-pole linkages (*1*), and the sensitivity of tropical regions to future climate change (*2*). High-resolution oxygen isotope records from Andean ice cores reveal the response of tropical mountain climates to global forcing during the Last Glacial Stage and Holocene (*2*). On Mt. Kenya, however, ice-core studies of the rapidly retreating mountain glaciers have proved unsuccessful because of meltwater percolation (*3, 4*). As an alternative, ^{18}O measurements can be made on diatom silica ($\delta^{18}O_{diatom}$) from the sediments of high-altitude lakes. A 3000-year $\delta^{18}O_{diatom}$ record obtained from Hausberg Tarn [4370 m above sea level (asl)], a glacier-fed lake on the northwest flank of Mt. Kenya (*5*), contained short-term minima in $\delta^{18}O_{diatom}$ attributed to glacier melting and longer term minima attributed to increased water temperatures (*5, 6*), in contrast to the positive relation assumed between $\delta^{18}O$ and air temperature in ice-core studies (*7*). Here, we present a 14,000-year $\delta^{18}O_{diatom}$ record compiled from two adjacent but hydrologically independent tarns located on the climatically sensitive northeast flank of Mt. Kenya. Their catchments have not been glaciated during the last 14,000 years (*6*).

Small Hall Tarn (SHT; 0°9′S, 37°21′E, 4289 m asl) is a topographically closed lake (0.5 m deep in January 1996) in the Gorges Valley. Simba Tarn (ST; 0°9′S, 37°19′E, 4595 m asl) is an open lake near the head of the Gorges Valley; in January 1996 it had a maximum depth of 5 m and an electrical conductance of just 18.9 $\mu S\ cm^{-1}$. Precipitation in the summit zone of Mt. Kenya falls mainly from March to May and in October and November, although some occurs in every month. Total precipitation declines with altitude above the tree line (~3000 m asl) and is <900 mm a^{-1} above 4500 m asl, where it mainly falls as snow (*3*). The main moisture source is the southwest Indian Ocean, because of southeasterly airflow in the lower troposphere during the rainy seasons (*3, 8*). Mean annual temperatures are close to freezing at both sites (+1.3°C at SHT, −0.7°C at ST), with a monthly variability of ±2°C but a large diurnal range (10° to 20°C) (*3*). Terrestrial plant cover is moderate (SHT) to very sparse (ST) at present.

Piston cores raised in 1996 from SHT and ST were dated by accelerator mass spectrometry, yielding 12 ^{14}C dates for SHT and 10 ^{14}C dates for ST (*9*). They were analyzed

[1]Hysed, Department of Geography, Lancaster University, Lancaster LA1 4YB, UK. [2]Tropical Palaeoenvironments Research Group, Department of Geography, University of Wales Swansea, Swansea SA2 8PP, UK. [3]Natural Environment Research Council (NERC) Isotope Geoscience Laboratory, Keyworth, Nottingham NG12 5GG, UK.

*Present address: Scottish Agricultural College, Crichton Royal Farm, Dumfries DG1 4SZ, UK.

†Present address: Department of Geography, University of Newcastle, Newcastle-upon-Tyne NE1 7RU, UK.

for volume magnetic susceptibility, diatoms, pollen, and green algae (SHT only) (*10*). Oxygen isotopes were measured on cleaned diatom silica from 72 levels in ST and 50 levels in SHT (*11*) (Figs. 1 and 2). Benthic, circumneutral, freshwater taxa, notably small *Fragilaria* spp., dominated the diatom assemblages. Changes in the diatom floras are coincident with isotope changes, but we do not observe systematic isotope-diatom species relations.

Strong agreement between the multiproxy data from SHT and ST enables us to identify two contrasting paleoenvironmental states. The first, characterized by stable, enriched $\delta^{18}O_{diatom}$ values (+27 to 37 per mil in SHT and +33 to 34 per mil in ST), corresponds to zones 1, 3, 5, and 7. Diatom-species richness

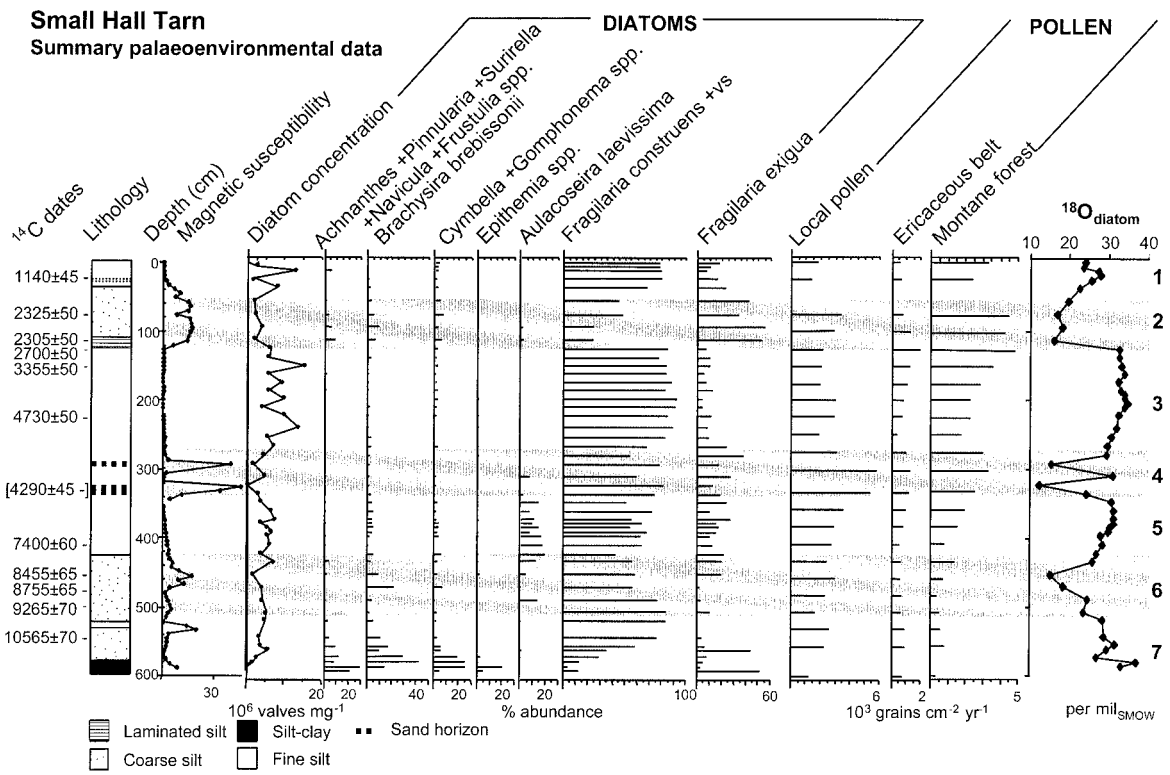

Fig. 1. Small Hall Tarn: summary of volume magnetic susceptibility, diatom analysis, pollen influx, and $\delta^{18}O_{diatom}$ data. Pollen taxa are grouped according to their modern distribution: local (Gramineae, Cyperaceae, *Alchemilla*, and Compositae), ericaceous belt, and montane forest (including dry, moist, and treeline species). The ^{14}C date in brackets was excluded from the age-depth model.

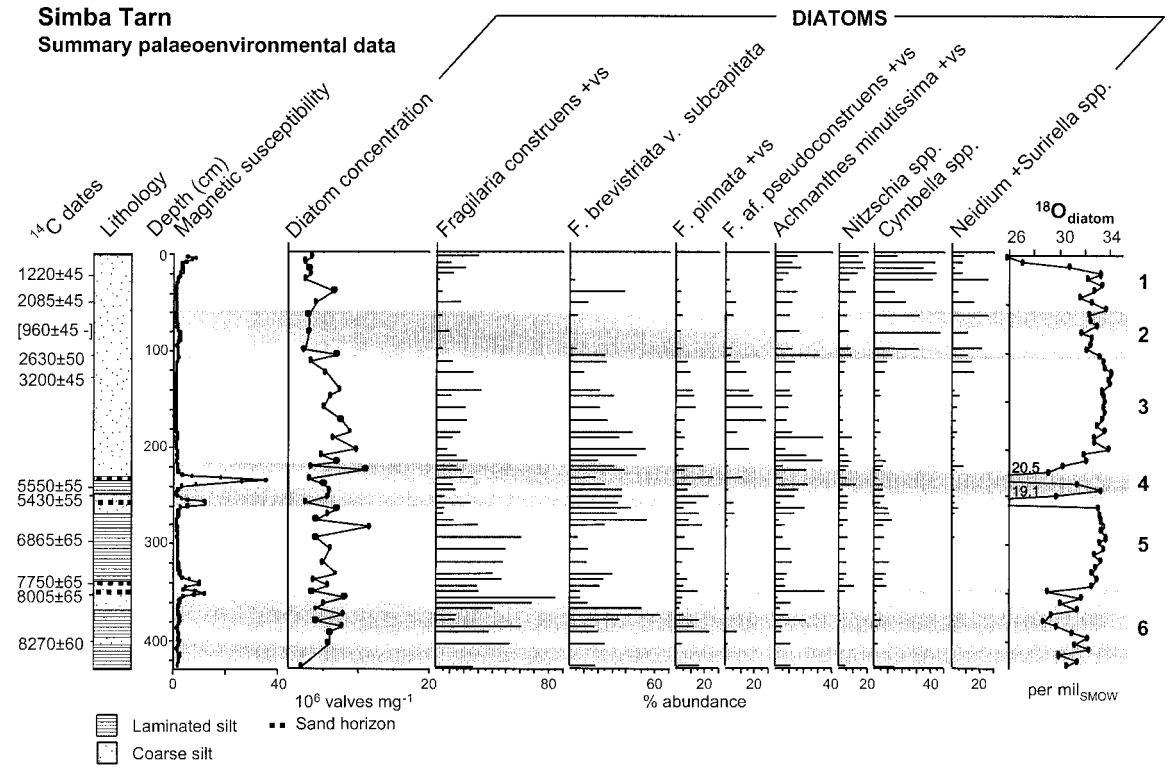

Fig. 2. Simba Tarn: summary of volume magnetic susceptibility, diatom analysis, and $\delta^{18}O_{diatom}$ data. The ^{14}C date in brackets was excluded from the age-depth model.

was generally greatest in these zones, particularly in the late-glacial sediments of SHT (zone 7). Here *Brachysira brebissonii*, a cold-water, oligotrophic species (*12*) found in the highest tarns on Mt. Kenya today, was codominant alongside the ubiquitous *Fragilaria* spp. Diversity was also high in zone 1 of Simba Tarn, suggesting an expansion of epiphytic niches available to the diatoms. Green algae, including *Pediastrum* and *Scenedesmus*, were most abundant during the periods of strongest isotopic enrichment in SHT.

The second paleoenvironmental state, characterized by more variable, strongly depleted $\delta^{18}O_{diatom}$ values, corresponds to zones 2, 4, and 6. In SHT, $\delta^{18}O_{diatom}$ values of <20 per mil occurred in all three zones; similar negative excursions are also found in ST, but only the changes in zone 4 are of comparable amplitude. High magnetic susceptibility values signifying allochthonous sediment influx are strongly correlated with isotopic depletion and low-diversity, *Fragilaria*-dominated diatom assemblages. Increased erosion of partially vegetated slopes may have created the turbid, disturbed habitats that *Fragilaria* readily occupy.

Influxes of pollen from terrestrial plants reflect changes in three major environmental variables: precipitation, temperature, and (at least during the late glacial period) atmospheric CO_2 pressure (*13*). Even-numbered isotope zones (depleted $\delta^{18}O_{diatom}$ values) correspond to modest increases in the influxes of local pollen (Gramineae, Cyperaceae, *Alchemilla*, and Compositae) together with montane-forest taxa transported from lower altitudes. Enhanced graminoid, shrub, and forest cover is consistent with wetter and/or warmer conditions.

During the last 14,000 years, four major negative shifts in $\delta^{18}O_{diatom}$ can be traced from basin to basin (Fig. 3). First, from 11.1 to 8.6 thousand years ago (ka), a decrease of 13 per mil was observed in SHT and 3 to 4 per mil in ST. Second, two abrupt $\delta^{18}O$ minima occurred between 6.7 and 5.6 ka. The amplitude of these isotopic excursions was 18 per mil in SHT and 14.2 per mil in ST. Third, a decrease in $\delta^{18}O_{diatom}$ occurred between 2.9 and 1.9 ka in all three isotope records from Mt. Kenya (Fig. 3). In SHT, $\delta^{18}O_{diatom}$ declined sharply by 16.6 per mil after 3.1 ka, whereas in ST this isotopic shift took place in two steps, ~3.4 ka and ~2.8 ka, giving a composite decrease of 2.5 per mil. In Hausberg Tarn the isotope signal was noisier, but the largest depletion of 2.3 per mil occurred at ~2.5 to 2.4 ka (*5*). Finally, the uppermost samples in SHT and ST show a substantial decrease of 3 per mil and 8 per mil, respectively, within the last 1.3 ka.

The similarity of the ST, SHT, and Hausberg Tarn isotope curves indicates underlying climate forcing modified by local hydrological factors. At tropical stations, the $\delta^{18}O$ values of monthly rainfall ($\delta^{18}O_{precip}$) exhibit a far stronger correlation with total precipitation (the "amount effect") than with air temperature (*14, 15*). By analogy with the Rayleigh-distillation model developed to explain seasonal variations in the isotopic values of surface snow on tropical ice caps (*16*), the main factors governing the isotopic composition of tropical alpine lakes are (i) the $\delta^{18}O$ value of the water vapor over the source region; (ii) the progressive rainout of the heavy isotope (^{18}O) along the air-mass trajectory from the source region, which is partially offset by recycling from the surface and evaporation of falling raindrops; (iii) orographic uplift; (iv) uplift in convective shower clouds; and (v) surface processes. In the case of lakes, the latter are dominated by evaporative enrichment of ^{18}O in lake water. Formation of diatom silica results in fractionation of the oxygen isotopes by around −0.2 to −0.5 per mil $°C^{-1}$ (*17*). Moreover, an increase in $^{18}O_{diatom}$ of 3 to 10 per mil has been reported during early diagenesis in ocean sediments (*18*).

Although insufficient data are available to quantify all these effects, the most important causes of isotopic variation can nevertheless be identified. General circulation model simulations for the Last Glacial Maximum suggest that the $\delta^{18}O$ values of rainfall ($\delta^{18}O_{precip}$) at low altitudes in the tropics were probably 1 to 3 per mil higher than today (*19, 20*): The net effect of a 1.6 per mil increase in the ^{18}O content of mean ocean water (*21*) is the lowering of tropical sea surface temperatures (SSTs), resulting in a smaller temperature gradient between the vapor source and the site of condensation, and hence the weakening of the African and Asian monsoons (reduced amount effect). The same factors would have contributed to the high values of $\delta^{18}O_{diatom}$ (maximum +36.7 per mil) recorded on Mt. Kenya during the late glacial period (14 to 11.2 ka).

Unfortunately, the modern isotopic composition of precipitation on Mt. Kenya is unknown, apart from spot dry-season measurements of ~ +0 to +2 per mil at 4200 m asl (*5*). However, $\delta^{18}O_{precip}$ values at Kericho (2130 m asl) and Muguga (2070 m asl) in the Kenya Highlands are ~ −4.4 and −3.8 per mil, respectively (*14*), the most negative isotopic values occurring during the wet seasons. The monthly $\delta^{18}O_{precip}$ values for these stations (*22*) lie close to the global meteoric line, indicating that precipitation formation occurs under isotopic-equilibrium conditions, with minimal evaporation of rainfall (*23*). For $\delta^{18}O$, the impact of orographic uplift is ~ −2.7 to −2.9 per mil km^{-1} in East Africa (*24*). This suggests that $\delta^{18}O_{precip}$ at our two study sites averages around −10 to −11.5 per mil. These estimates are compatible with spot measurements of –9 per mil on river runoff from 4000 m asl (*24*), –8 per mil on surface snow from the Lewis Glacier (*4*), –6 to –7 per mil on Hausberg and Oblong Tarns (open lakes fed by glacial meltwater), and +1 per mil on Naro Moru Tarn (a closed lake) (*5*).

During wetter intervals in the past, the mean isotopic values of lake water would have been lowered by increases in precipitation (*14, 16, 25*) and cloud height [giving lower cloud-top temperatures (*23, 26*)], strongly reinforced by decreased evaporation and possibly by lake overflow (in the case of SHT). Note, however, that any reduction in water temperatures resulting from increased cloud would have partially counteracted these effects through its impact on isotopic fractionation by diatoms.

A comparison of the Holocene variations in $\delta^{18}O_{diatom}$ (Fig. 3) with alkenone SST estimates for the southwest tropical Indian Ocean, the source of much of the precipitation on Mt. Kenya, shows that the isotopic minima around 9 ka and at 6.9 to 5.8 ka corresponded to high SSTs (*27*). At present, heavy seasonal rainfall totals over the eastern Kenya Highlands are strongly linked to pos-

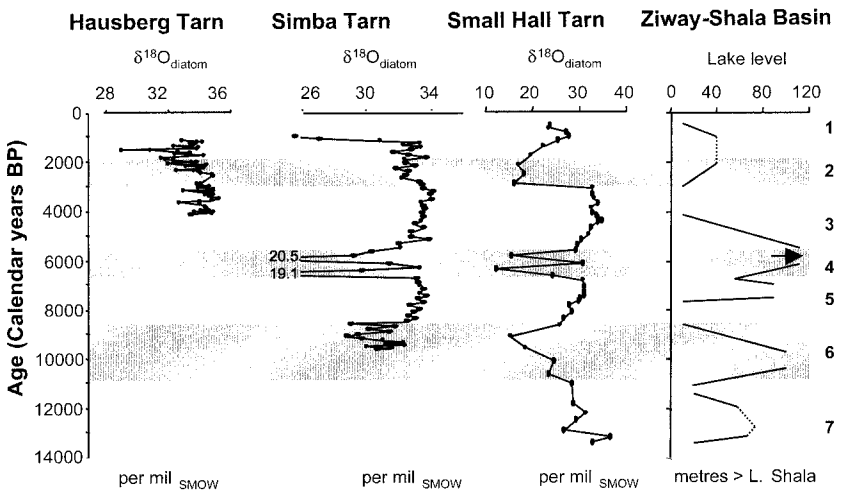

Fig. 3. Isotope data from Simba Tarn, Small Hall Tarn, and Hausberg Tarn (*5*). These data are compared to lake levels in the Ziway-Shala Basin, Ethiopia, derived from ^{14}C-dated shorelines (*32*).

itive SST anomalies over the tropical South Atlantic and Indian Oceans, as well as to El Niño–Southern Oscillation events (*28*). The heavy rains of 1961–1962 provide a modern analog for the abrupt, high-amplitude $\delta^{18}O_{diatom}$ minima. In November 1961, for example, the precipitation on the footslopes of Mt. Kenya exceeded 275% of normal (*28*) as a result of onshore flow from a large area of anomalously warm SSTs in the western Indian Ocean. Evaporation was also greatly reduced by dense cloud (*29*). A 145-year tree-ring study from Narok Mau, Kenya, confirms a 30 per mil decrease in mean δD, which is highly correlated with $\delta^{18}O$ (*24*) from 1953–1958 to 1959–1963 (*30*).

The importance of moisture balance in causing the $\delta^{18}O_{diatom}$ minima is supported by the pollen evidence for wetter and/or warmer conditions (Fig. 3). Notwithstanding a modest increase in plant cover, unusually heavy precipitation may have led to severe erosion of exposed volcanic soils on Mt. Kenya (*31*), resulting in the magnetic-susceptibility peaks. Our data suggest that anomalously heavy snowfall on the peaks of Mt. Kenya may contribute to the neoglacial ice advances dated >5.7 ka, 3.2 to 2.3 ka, and 1.3 to 1.2 ka (*6*). Lake-level curves from the East African–South Asian monsoon region (*32, 33*) support our climatic interpretation of the $\delta^{18}O_{diatom}$ data (Fig. 3), as does pollen evidence for generally wetter and warmer conditions in Kenya at ~6.8 ka (*34*). Environmental changes on Mt. Kenya are therefore symptomatic of the same climatic-forcing mechanisms that affected low-altitude tropical areas.

We conclude that centennial- to millennial-scale fluctuations in the ^{18}O content of diatom silica from alpine lakes on Mt. Kenya primarily reflect variations in moisture balance and cloud height, driven by SST anomalies. Hence, they provide a valuable new data source to supplement the sparse and rapidly deteriorating (*7*) isotopic archives in tropical glaciers.

References and Notes

1. J. C. Stager, P. A. Mayewski, *Science* **276**, 1834 (1997).
2. L. G. Thompson *et al*., *Science* **282**, 1858 (1998).
3. S. Hastenrath, *The Glaciers of Equatorial East Africa* (Reidel, Dordrecht, Netherlands, 1981).
4. L. G. Thompson, in *Sea Level, Ice and Climatic Change*, I. Allison, Ed. (IAHS, Canberra, 1979), vol. 131, pp. 55–64.
5. M. Rietti-Shati, A. Shemesh, W. Karlén, *Science* **281**, 980 (1998).
6. W. Karlén *et al*., *Ambio* **28**, 409 (1999).
7. L. G. Thompson, E. Mosley-Thompson, K. A. Henderson, *J. Quat. Sci.* **15**, 377 (2000).
8. C. K. Gatebe, P. D. Tyson, H. Annegarn, S. Piketh, G. Helas, *J. Geophys. Res.* **104**, 14237 (1999).
9. The ^{14}C dates were measured on total organic carbon and calibrated to give calendar ages using CALIB 3.0. A table of ^{14}C dates is available at *Science* Online (www.sciencemag.org/cgi/content/full/292/5525/2307/DC1). The chronology has been interpolated using a third-order polynomial regression model. For SHT, the regression equation is $y = 0.00006x^3 - 0.039x^2 + 24.747x + 524.2$, $r^2 = 0.994$, and for ST, $y = 0.00012x^3 + 0.071x^2 + 11.227x + 1041.2$, $r^2 = 0.996$, where x is core depth (cm) and y is calendar age before the present. The mud-water interface was not recovered, and ages above the youngest ^{14}C date should be treated with caution.
10. Standard methods were used for the analysis of diatoms, pollen, and magnetic susceptibility (*13*). See also D. L. Swain, thesis, University of Wales, Swansea (1999).
11. Diatom silica was concentrated (to >98%) by chemical cleaning, sieving, and differential settling. The determination of $\delta^{18}O_{diatom}$ included outgassing and prefluorination, followed by extraction of the inner tetrahedrally bound oxygen by a fluorination method. The results were calibrated against laboratory diatom-standard materials and NBS28 international standard quartz, and are reported against Vienna standard mean ocean water (VSMOW). Samples were analyzed up to three times, giving a mean reproducibility of ±0.3 per mil at 1σ. The laboratory diatom standard had a mean variance of ±0.3 per mil, and standard NBS28 had a variance of ±0.1 per mil (both at 1σ), over the period of analysis.
12. W. Vyverman, K. Sabbe, *J. Paleolimnol.* **13**, 65 (1995).
13. F. A. Street-Perrott *et al*., *Science* **278**, 1422 (1997).
14. K. Rozanski, L. Araguas-Araguas, R. Gonfiantini, in *Climate Change in Continental Isotopic Records*, P. K. Swart, K. C. Lohmann, J. McKenzie, J. Savin, Eds. (American Geophysical Union, Washington, DC, 1993) pp. 1–36.
15. K. Rozanski, L. Araguas-Araguas, R. Gonfiantini, in *The Limnology, Climatology and Paleoclimatology of the East African Lakes*, T. C. Johnson, E. O. Odada, Eds. (Gordon and Breach, Amsterdam, 1996), pp. 79–93.
16. P. M. Grootes, M. Stuiver, L. G. Thompson, E. Mosley-Thompson, *J. Geophys. Res.* **94**, 1187 (1989).
17. M. E. Brandriss, J. R. O'Neil, M. B. Edlund, E. F. Stoermer, *Geochim. Cosmochim. Acta* **62**, 1119 (1997).
18. M. Schmidt *et al*., *Geochim. Cosmochim. Acta* **65**, 201 (2001).
19. G. Hoffmann, M. Heimann, *Quat. Int.* **37**, 115 (1997).
20. J. Jouzel, G. Hoffmann, R. D. Koster, V. Masson, *Quat. Sci. Rev.* **19**, 363 (2000).
21. J. Duplessy, J. Moyes, C. Pujol, *Nature* **286**, 479 (1980).
22. International Atomic Energy Agency and World Meteorological Organisation, *Global Network for Isotopes in Precipitation (GNIP) and Isotope Hydrology Information System (ISOHIS)* (http://isohis.iaea.org).
23. R. Njitchoua *et al*., *J. Hydrol.* **223**, 17 (1999).
24. W. G. Darling, thesis, Open University (1996).
25. L. G. Thompson, S. Hastenrath, B. M. Arnao, *Science* **203**, 1240 (1979).
26. J.-C. Fontes, F. Gasse, J. Andrews, in *Isotopic Techniques in the Study of Past and Current Environmental Changes in the Hydrosphere and Atmosphere* (International Atomic Energy Agency, Vienna, 1993), pp. 231–248.
27. C. Sonzogni, E. Bard, F. Rostek, *Quat. Sci. Rev.* **17**, 1185 (1998).
28. S. E. Nicholson, in *The Limnology, Climatology and Paleoclimatology of the East African Lakes*, T. C. Johnson, E. O. Odada, Eds. (Gordon and Breach, Amsterdam, 1996), pp. 25–56.
29. H. Flohn, *Palaeoecol. Afr.* **18**, 3 (1987).
30. R. V. Krishnamurthy, S. Epstein, *Nature* **317**, 160 (1985).
31. W. M. Ngecu, E. M. Mathu, *Environ. Geol.* **38**, 277 (1999).
32. F. A. Street-Perrott, R. A. Perrott, *Nature* **343**, 607 (1990).
33. F. Gasse, E. Van Campo, *Earth Planet. Sci. Lett.* **126**, 435 (1994).
34. O. Peyron, D. Jolly, R. Bonnefille, A. Vincens, J. Guiot, *Quat. Res.* **54**, 90 (2000).

35. Supported by NERC grant GR3/A9523, radiocarbon allocation 728/1297, and isotope project IP/565/0998. Permission for fieldwork in Kenya was granted by the Office of the President, Nairobi, and supported by the National Museum of Kenya. We thank S. Hastenrath, F. Gasse, and an anonymous reviewer for their constructive comments.

6 February 2001; accepted 21 May 2001

Paleobotanical Evidence for Near Present-Day Levels of Atmospheric CO_2 During Part of the Tertiary

Dana L. Royer,[1]*† Scott L. Wing,[2] David J. Beerling,[3] David W. Jolley,[4] Paul L. Koch,[5] Leo J. Hickey,[1] Robert A. Berner[1]

Understanding the link between the greenhouse gas carbon dioxide (CO_2) and Earth's temperature underpins much of paleoclimatology and our predictions of future global warming. Here, we use the inverse relationship between leaf stomatal indices and the partial pressure of CO_2 in modern *Ginkgo biloba* and *Metasequoia glyptostroboides* to develop a CO_2 reconstruction based on fossil *Ginkgo* and *Metasequoia* cuticles for the middle Paleocene to early Eocene and middle Miocene. Our reconstruction indicates that CO_2 remained between 300 and 450 parts per million by volume for these intervals with the exception of a single high estimate near the Paleocene/Eocene boundary. These results suggest that factors in addition to CO_2 are required to explain these past intervals of global warmth.

Atmospheric CO_2 concentration and temperature have been tightly correlated for the past four Pleistocene glacial-interglacial cycles (*1*). Various paleo-CO_2 proxy data (*2, 3*) and long-term geochemical carbon cycle models (*4–6*) also suggest that CO_2-temperature coupling has, in general, been maintained for the entire Phanerozoic (*7*). Recent CO_2 proxy data, however, indicate low CO_2 values during the mid-Miocene